- Technical Paper -

Sensitivity analysis on the impact of aggregate and ITZ strength on the concrete properties by RBSM

Hiroshi SASANO[*1], Ippei MARUYAMA[*2]

ABSTRACT

A three-phase mesoscale model for concrete (mortar-interfacial transition zone (ITZ)-aggregate) has been developed using a rigid body spring model (RBSM), and a sensitivity analysis of the aggregate strength and the ITZ strength in tension and compression was conducted. It was found that the aggregate strength had a significant impact on the compressive strength and its post-peak behavior: as the aggregate strength increased, the concrete compressive strength increased while the tensile splitting strength was changed little by the aggregate strength. Furthermore, the ITZ strength affected both the compressive strength and the tensile splitting strength in proportion to ITZ strength. In this study, experimental results were reproduces using 150 MPa as the aggregate strength, and 62.5 % of the mortar strength as the strength of ITZ.

Keywords: Concrete properties, Rigid body spring model, three-layer model, Aggregate strength, ITZ

1. INTRODUCTION

Some concrete deterioration is brought about by the physical interaction between mortar and aggregate: e.g. Young's modulus reduction due to drying-induced microcracks[1], reduction in Young's modulus and strength due to neutron irradiation and resultant aggregate metamictization[2], an alkali-silica reaction (ASR), and delayed ettringite formation (DEF).

For the aging management of concrete structures, evaluating and predicting the concrete properties of existing structures is essential. Therefore, we attempt to develop a numerical model which can reproduce these deteriorations caused by interaction between aggregate and mortar. In the present paper, calibration of concrete before degradation is reported.

To analyze these deteriorations, we adopted a three-phase model of concrete: mortar, aggregate, and interface (ITZ). Because a three-phase model deals with physical interaction among them directly, that is: a concrete element model with aggregate and mortar averaged cannot deal with these phenomena directly. Although the three-phase model has many parameters to calibrate, this model can be applied in other conditions such as the anisotropy of cracks under restraint condition without any special consideration as well as can deal with the interaction between mortar and aggregate.

However, the three-phase concrete model for numerical analysis has not been established sufficiently. Many types of research have been contributed to this field so far [3-6]. However, ITZ properties are different in each model, and many numerical models assume an aggregate is elastic although aggregates break as shown in Fig. 1. In Fig. 1, fracture of some aggregate was observed after compressive test [1].

For this reason, a parametric study on both the strength of ITZ and the strength of aggregate were conducted. Furthermore, from the parametric study results, impacts of the ITZ strength and the aggregate strength on both the compressive strength and the tensile splitting strength of concrete were investigated.

2. NUMERICAL MODEL

2.1 RBSM

In this study, the Rigid Body Spring Model (RBSM), developed by Kawai [7], was adopted. As shown in Fig. 2, The RBSM employs a discrete numerical analysis method, and deals with the crack propagation of concrete directly, since the RBSM represents a continuum material as an assembly of rigid particle

Fig. 1 Fracture condition of G2 aggregate**[1]**

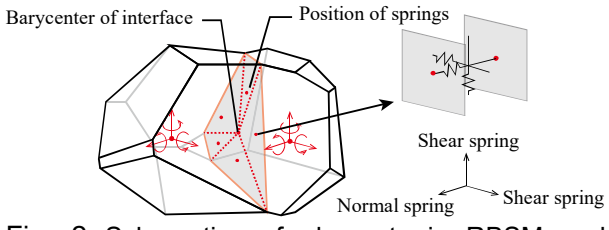

Fig. 2 Schematics of elements in RBSM and springs connecting rigid bodies

*1 Ph.D. student, Dept. of Environmental Eng. and Arch., Nagoya University, JCI Student Member
*2 Professor Dept. of Environmental Eng. and Arch., Nagoya University, Dr.Eng., JCI Member

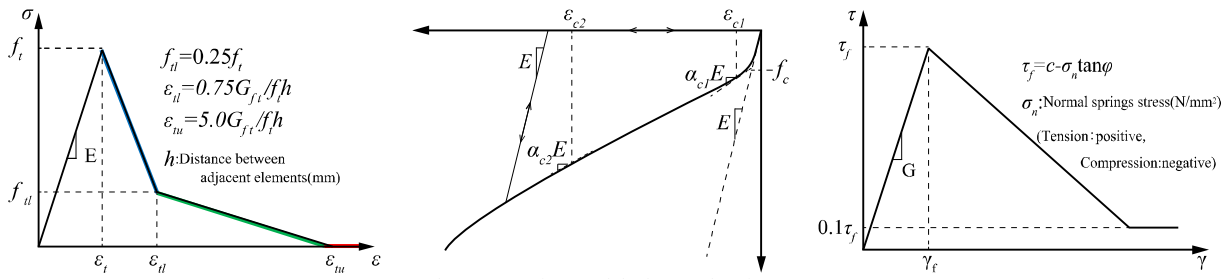

(a)Tensile model of normal spring (b)Compression model of normal spring (c) Shear spring model

Fig. 3 Constitutive models for concrete

Table 1 Mixture properties of target experiment ([1], [11])

	W/C (%)	Air (%)	Unit mass (l/m^3)				S/(Air+W+C+S)
			W	C	S	G	
Compressive	55	2.6	160	93	332	375	0.54
Tensile		4.0	177	102	363	338	0.53

elements interconnected by springs along their boundaries. Based on the nonlinear behavior of these springs, the cracking behavior of a continuum material can be simulated. In this model, each integral point has one vertical spring and two tangential springs (the direction of the two tangential springs are the direction of x- and y-axes when the z-axis of the global coordinate system is rotated to match the normal vector of the surface).

(1) Mortar model

Fig. 3 shows a constitutive model of a mortar element. For the tensile behavior of mortar, a bilinear softening branch of a 1/4 model was adopted, and for the compressive behavior, reversed S-shape constitutive low, which does not show softening, was applied.

Regarding tangential springs, the Mohr-Coulomb type criterion was adopted for shear strength, and the softening gradient was changed according to the normal spring stress. In other words, depending on the stress of normal spring, the stress-strain relationships of shear spring changes. For further information, such as the sensitivity analysis of the spring parameters, this paper [8] and [9] are available.

(2) Aggregate model

The same constitutive low as the mortar was adopted.

(3) Mortar-aggregate interface model (ITZ model)

As many researchers have reported, the porosity around the aggregate is higher than the bulk mortar due to the "wall effect" of aggregate [10]. Consequently, lower physical properties (e.g., tensile strength, cohesive strength, Vickers hardness) is observed.

Hence, a constitutive low for ITZ was developed as shown in Fig. 4. In tension field, Young's modulus (E_{c_ITZ}) and tensile strength (f_{t_ITZ}), fracture energy (G_{ft_ITZ}) were determined by following equations.

$$E_{c\_ITZ} = \alpha E_{cm} \quad (1)$$

$$f_{t\_ITZ} = \beta f_{tm}, G_{ft\_ITZ} = \beta G_{ftm}, c_{ITZ} = \beta c_m \quad (2)$$

where α, β: coefficient ($0<\alpha$, $\beta<1.0$), E_{cm}: Young's modulus of mortar, f_{tm}: tensile strength of mortar, G_{tfm}: tensile fracture energy of mortar, c_m: cohesive strength of mortar. In compression field, until reaching the strain equivalent to ITZ thickness (ε_{ITZ}), Young's modulus

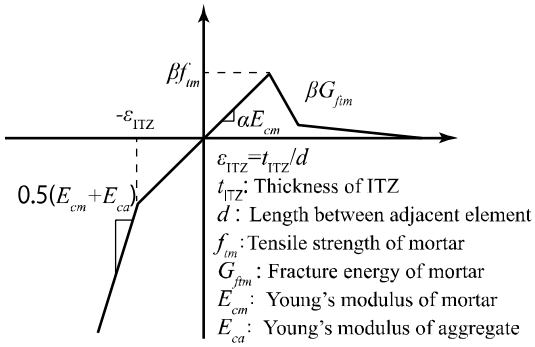

Fig. 4 Constitutive low of mortar-aggregate interface

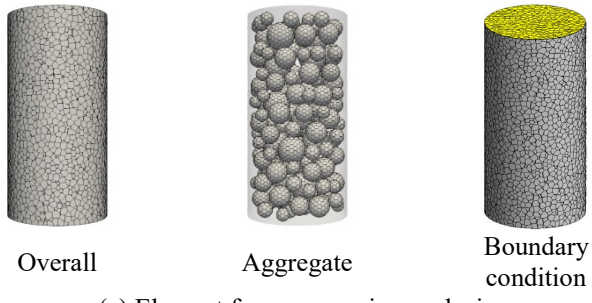

(a) Element for compressive analysis

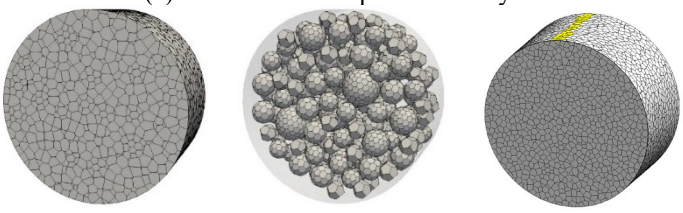

(b) Element for tensile splitting analysis

Fig. 5 Concrete meshes for analysis

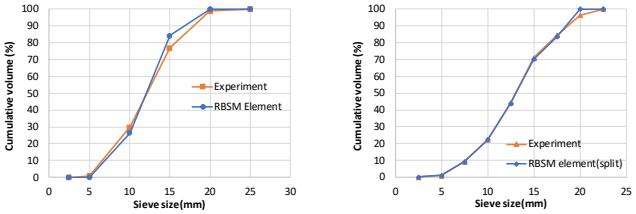

(a) For compressive test (b)For tensile splitting test

Fig. 6 Particle distribution of aggregate

was same as tension field, after exceeding ε_{ITZ}, average Young's modulus of mortar and aggregate was adopted.

In the shear field, like the tension field, shear modulus and shear strength (i.e., cohesive strength) (c_{ITZ}) were determined by equation (2).

2.2 Outline of the analysis

(1) Target experiment

As target experiments, researches of Maruyama, Sasano [1] and Lin, Itoh [11] were selected. In the former research, the compressive test of the ϕ 5x10cm specimen was conducted, and in the latter, the tensile splitting test of the ϕ 10x1cm specimen was carried out.

Table 1 shows the mixture properties of target specimens. Both samples use the sand of the same production area, and the mixture properties of the mortar in concrete were almost the same.

(2) Element

Fig. 5 shows meshes for analysis. The meshes which shape are φ5x10cm and φ10x5cm were prepared for compressive analysis and tensile splitting analysis respectively. Both the meshes were created using the Voronoi diagram to reduce the element dependency of crack patterns [12]. Boundary conditions were introduced to the yellow elements in Fig. 5 (similar conditions were also set to the bottom surface). For the compressive analysis, plate elements were attached to the colored surface, and displacement was given to the plate. While, for the tensile splitting analysis, displacement was given to the colored elements directly.

The volume fraction of aggregate in RBSM mesh was 36.05% (37.5% in Experiment) for the compressive test and 33.84% (33.8% in Experiment) for splitting test. Fig. 6 shows the particle distribution of aggregate. From the above, the volume fraction and the particle distribution of RBSM mesh are almost the same as the experiment.

In the mesh for the compressive test, mesh size was 2.09mm on average, and the total number of elements was 35570, the number of aggregate elements was 18643. In the mesh for the tensile splitting test, mesh size was 2.96mm on average, and the total number of elements was 27381, the number of aggregate elements was 12375.

(3) Materials and spring properties

Table 2 shows material properties measured or calculated from experimental results. Regarding Young's modulus (E_c), tensile strength (f_t), compressive strength(f_c) of mortar, items which were not measured were calculated from the following equations.

$$f_{tm} = 1.91Ln(f_{cm}) - 3.85 \quad (3)$$

$$E^*_{cm}(f_{cm}) = 0.185f_{cm} + 14.6 \quad (4)$$

$$E_{cm} = 16900 \cdot E^*_{cm}(f_{cm})/E^*_{cm}(46.6) \quad (5)$$

where f_{tm} is splitting tensile strength of mortar; f_{cm} is compressive strength of mortar; E^*_{cm}, E_{cm} are Young's modulus of mortar. As shown in Fig. 7, Equation (3), (4) were made from Kosaka, Tanigawa [13] experimental results. Then, according to Equation (5), E^*_{cm} was corrected to E_{cm} to match the experimental results [1] ("19600" and "46.6" in Equation(5) are E_c and f_c of Mortar-C in Table 2 respectively). Moreover, fracture energy (G_{ft}) of mortar was calculated following the JSCE [14] formula.

Table 2 Applied values of springs in the numerical calculation

	E_c (N/mm^2)	f_t (N/mm^2)	f_c (N/mm^2)	G_{ft} (N/mm)
Mortar-C	16900[1)]	3.49[4)]	46.6[1)]	0.0615[3)]
Aggregate-C	70000[1)]	7.00[5)]	100～250[6)]	0.0005[5)]
Mortar-T	17800[4)]	3.76[2)]	52.8[4)]	0.0644[3)]
Aggregate-T	70000[1)]	7.00[5)]	150, 250[6)]	0.0005[5)]

C: for compressive test, T: for tensile splitting test

1) Maruyama, Sasano [1], 2) Lin *et al.* [11], 3) JSCE formula [14], 4) Kosaka *et al.* [13], 5)Sufficiently small/large comparing with mortar, 6) sensitive analysis parameter (see in Table 4)

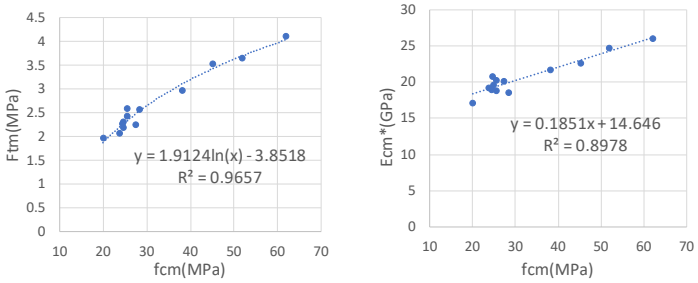

(a) f_{cm}-f_{tm} (b) f_{cm}-E^*_{cm}

Fig. 7 Relationships of material properties

Table 3 Applied values of springs in the numerical calculation

(a) Normal spring

Young's modulus	Tension field		Compression field			
E_c (N/mm^2)	f_t (N/mm^2)	G_{ft} (N/mm)	f_c (N/mm^2)	ε_{c2}	α_{c1}	α_{c2}
$1.6E_c^*$	$1.4f_t^*$	$1.5G_{ft}^*$	$1.5f_c^*$	-0.015	0.15	0.25

(b) Shear spring

Shear modulus	Failure criteria			Softening behavior			
$\eta=G/E_c$	c (N/mm^2)	φ (degree)	σ_b (N/mm^2)	β_0	β_{max}	χ	κ
0.42	$0.14f_c^*$	37	$0.55f_c^*$	-0.05	-0.025	-0.01	-0.3

Table 4 Notation and parameters for numerical analysis

Objective	Test type[1)]	Notation	Aggregate f_c (MPa)	ITZ properties[2)] $E_{c\ ITZ}$	$f_{t\ ITZ}$	$G_{ft\ ITZ}$	c_{ITZ}
Impact of aggregate strength on concrete properties	C	Agg-Fc=100	100	$0.5E_{cm}$	$0.5f_{tm}$	$0.5G_{ftm}$	$0.5c_m$
	C	Agg-Fc=120	120				
	C・T	Agg-Fc=150	150				
	C・T	Agg-Fc=250	250				
Impact of ITZ strength on concrete properties	C・T	ITZ=0.25	150	$0.5E_{cm}$	$0.25f_{tm}$	$0.25G_{ftm}$	$0.25c_m$
	C・T	ITZ=0.5		$0.5E_{cm}$	$0.5f_{tm}$	$0.5G_{ftm}$	$0.5c_m$
	C・T	ITZ=0.625		$0.5E_{cm}$	$0.625f_{tm}$	$0.625G_{ftm}$	$0.625c_m$
	C・T	ITZ=0.75		$0.5E_{cm}$	$0.75f_{tm}$	$0.75G_{ftm}$	$0.75c_m$

[1)]C: compressive test, T: tensile splitting test, [2)]E_{cm}, f_{tm}, G_{ftm}, c_m: mortar properties (subscript "m" means mortar)

$$G_{ftm} = 0.01 \cdot (d_{max})^{\frac{1}{3}} \cdot f_{cm}{}^{\frac{1}{3}} \quad (6)$$

where, G_{ftm}: fracture energy of mortar (N/mm), d_{max}(=5mm): maximum grain size of the aggregate (mm)

Table 3 shows the relationship between physical properties and springs properties in RBSM. Since in the RBSM, unlike FEM, spring properties do not have physical meanings, each parameter in has been decided by conducting parametric analyses comparing the specimen test results of the tensile splitting test, the uniaxial compression test following the previous research [8].

(4) The ITZ properties and the parameter for numerical analysis

Parameters for numerical studies were shown in Table 4. The objective of the present study is investigating the impact of aggregate and ITZ strength. Therefore, analysis under four types of aggregate strength (100, 120, 150, 250 MPa) and four types of ITZ strength (25%, 50%, 62.5%, 75% of the mortar strength) were conducted. Young's modulus of ITZ was fixed as 50% of Young's modulus of the mortar.

3. RESULTS

3.1 Impact of Aggregate strength

(1) Compressive strength

Fig. 8 shows stress-strain relationships of the experimental results and the compressive loading analysis with varying strength of aggregate. Table 5 lists the numerical results of the compressive strength and the tensile splitting strength. From Fig. 8, as aggregate strength increased, compressive increased. Moreover, Agg-Fc=250 and Agg-Fc=150 are close to the experimental result (96.8 %, 94.8% of experimental result respectively).

On the other hands, as the aggregate strength increased, the higher stress at a given strain in the post-peak was observed. Taking into account the post-peak behavior, aggregate strength of 150 MPa (Agg-Fc=150) was the most

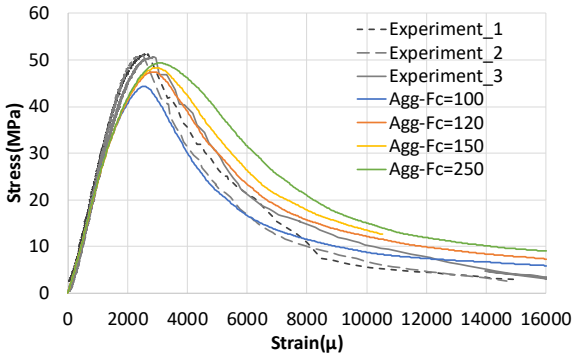

Fig. 8 Effect of aggregate strength on the stress-strain relationships

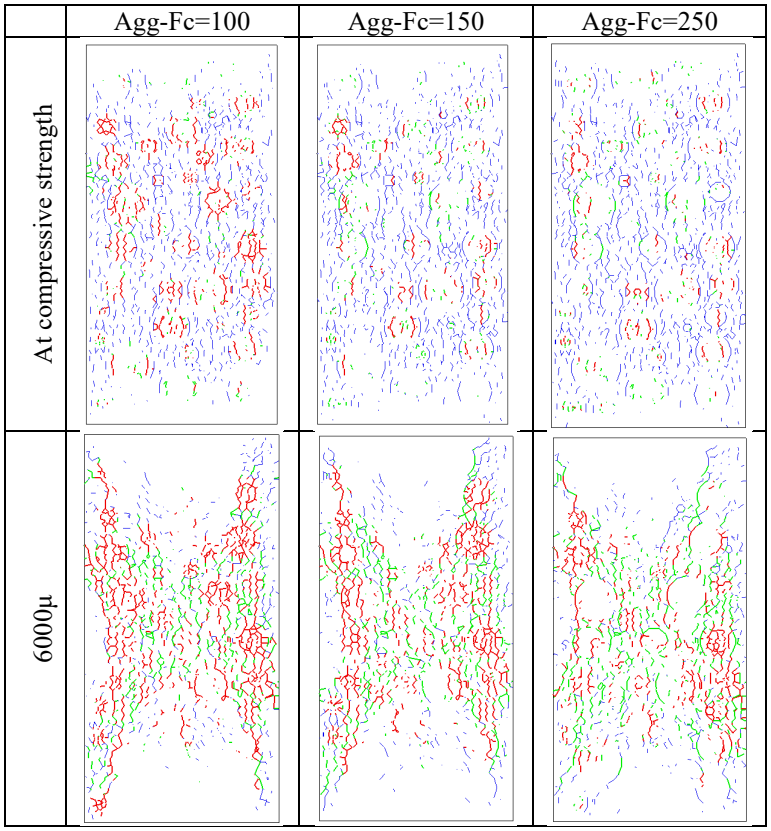

Fig. 9 Crack patterns of compressive loading: Aggregate strength

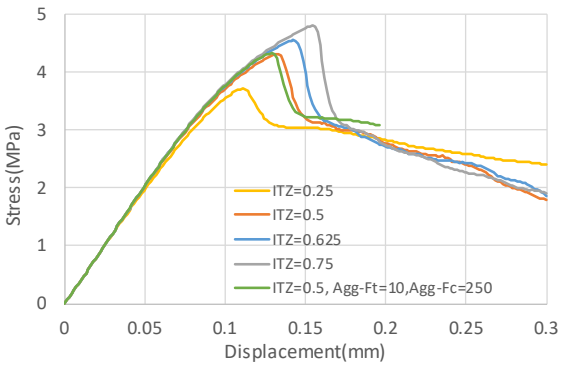

Fig. 12 Stress-strain relationships with varying ITZ strength

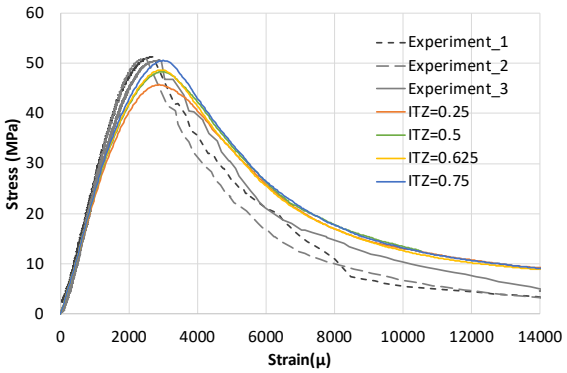

Fig. 13 Effect of ITZ strength on the stress-strain relationships

appropriate parameter. Hence, we adopted the aggregate strength of 150 MPa for sensitivity analysis of ITZ.

The underlying mechanism of the above-described results needs to be discussed. Fig. 9 shows crack patterns of the compressive loading analysis at the maximum load and the strain of 6000μ (post-peak). The colors in Fig. 9 is related to the color in Fig. 3(a) (When the maximum historical strain of a vertical spring is on the blue line, and the current strain is in tension fields, the faces is painted in blue). At the compressive strength, more aggregates fractured in Agg-Fc=100 than both Agg-Fc=150 and Agg-Fc=250. Also, a similar crack pattern was observed between Agg-Fc=150 and Agg-Fc=250. At 6000μ, the aggregates fracture developed, and a corn shape crack pattern was observed similarly as during a compression experiment. Besides, the number of cracks in Agg-Fc=250 was smaller than Agg-Fc=100 and Agg-Fc=150 due to the higher strength of aggregate.

From these results, it was concluded that the aggregate of higher strength restrained the crack development led to the higher compressive strength and less softening behavior.

(2) Tensile splitting strength

Stress-displacement relationships of tensile splitting analyses are shown in Fig. 10. Comparing "ITZ=0.5" and "ITZ=0.5, Agg-Ft=10, Agg-Fc=250", the aggregate strength has little influence on the tensile splitting strength.

To summarize, it was concluded that aggregate strength has a significant influence on the compressive strength and its softening behavior, and little impact on the tensile splitting strength. Therefore, it should be noted that in some cases such as when the mortar strength is close to the aggregate strength, introducing of aggregate fractural behavior is suitable rather than assuming that aggregate is elastic.

3.2 Impact of ITZ properties

Fig. 10 and Fig. 11 show the stress-strain/displacement relationships of the tensile and compressive analysis with different ITZ strength

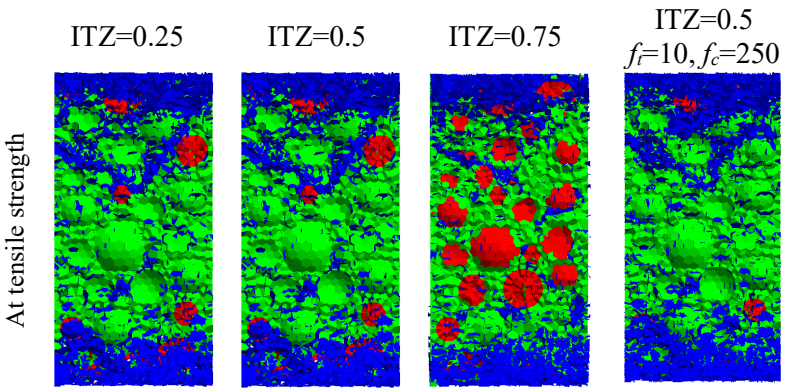

Fig. 10 Fracture surface in concrete after tensile splitting analysis

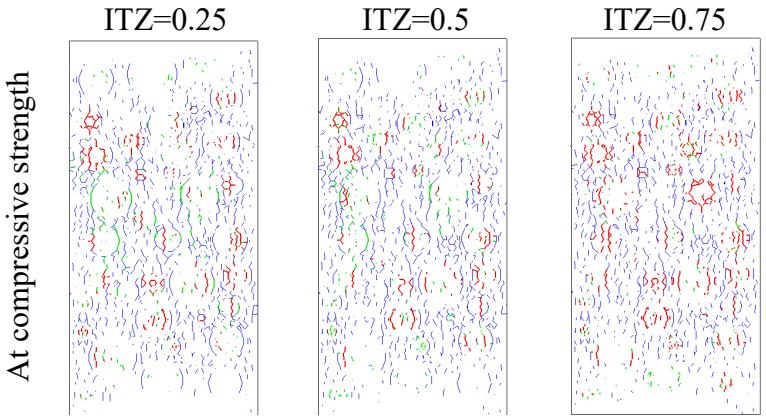

Fig. 11 Crack patterns of compressive loading: ITZ strength

respectively. In both tension and compression, as the ITZ strength increased, both the tensile and the compressive strength increased. Notably, the ITZ strength significantly affected the tensile strength (see in Table 5). These strengths increases were almost linearly proportional with the ITZ strength.

The crack pattern from the tensile analysis is shown in Fig. 12. In these 3D pictures, the cracks are seen from the side of the mesh at the maximum load. ITZ=0.25, 0.5 showed almost the same crack pattern, while more aggregate fracture was observed in ITZ=0.75. Fig. 13 shows the crack patterns during compressive analysis with varying ITZ strength. In compressive loading, ITZ=0.25, 0.5 showed the same crack behavior, while ITZ=0.75 showed more fractured aggregate than the former two. The changes in crack behavior were not significant.

Table 5 Summary of the parametric study

		Aggregate strength (MPa)				ITZ strength coefficient: β (-)			
		100	120	150	250	0.25	0.5	0.625	0.75
Analysis	σ_c	44.4	47.4	48.3	49.4	45.7	48.3	49.0	50.5
(MPa)	σ_t	-	-	4.31	4.33	3.71	4.31	4.55	4.80
Comparison	σ_c/f_c	87.0	93.0	94.8	96.8	89.6	94.8	96.1	99.1
with Exp. (%)	σ_t/f_t	-	-	97.2	97.5	83.6	97.2	102.6	108.1

σ_c, σ_t: Maximum load of the compressive/tensile splitting analysis, f_c, f_t: the compressive/tensile splitting strength of the experiment

3.3 Summary of sensitive analysis

All analysis results were summarized in Table 5. According to these results and softening behavior (see in Fig. 8), aggregate strength of 150 MPa and ITZ strength of 62.5 % of mortar gave the best match to the experimental results.

4. CONCLUSIONS

In this study, a three-phase mesoscale model for concrete (mortar-ITZ-aggregate) has been developed using a rigid body spring model (RBSM), and a sensitivity analysis on aggregate strength and the strength of ITZ both in tension and compression was conducted. The results were as follows:

(1) Aggregate strength had a significant impact on the concrete strength and post-peak softening behavior. As the aggregate strength increased, the compressive strength increased, and the lesser softening behavior was observed. From the crack patterns, these phenomena can be explained by the restraining effect of the higher-resistant aggregate to the crack development.

(2) The aggregate strength had little impact on the tensile splitting strength.

(3) ITZ strength affected both the compressive and the tensile splitting strength. This strength change was almost linear with the strength of ITZ. In the case of the tensile splitting analysis, it was confirmed that the higher strength of ITZ increased the number of aggregate cracks.

(4) In this study, the aggregate strength of 150 MPa and the ITZ strength of 62.5 % of mortar gave the best match to the experimental results.

(5) Conclusions (1) implies that assuming aggregate is elastic in the analysis may overestimate the strength especially if the mortar strength is close to the aggregate strength.

ACKNOWLEDGEMENT

This work was supported by METI Energy of “Technical development for a common basis of nuclear safety.”

REFERENCES

[1] Maruyama, I., *et al.*, "Strength and Young's modulus change in concrete due to long-term drying and heating up to 90°C," Cement and Concrete Research, Vol.66, 2014, pp. 48-63

[2] Maruyama, I., *et al.*, "Development of Soundness Assessment Procedure for Concrete Members Affected by Neutron and Gamma-Ray Irradiation," Journal of Advanced Concrete Technology, Vol.15, No.9, 2017, pp. 440-523

[3] Nagai, K., Sato, Y., and Ueda, T., "Mesoscopic simulation of failure of mortar and concrete by 3D RBSM," Journal of Advanced Concrete Technology, Vol.3, No.3, 2005, pp. 385-402

[4] Zhang, S., *et al.*, "Numerical study of the effect of ITZ on the failure behaviour of concrete by using particle element modelling," Construction and Building Materials, Vol.170, 2018, pp. 776-789

[5] Caballero, A., Carol, I., and LÓPez, C.M., "A meso‐level approach to the 3D numerical analysis of cracking and fracture of concrete materials," Fatigue & Fracture of Engineering Materials & Structures, Vol.29, No.12, 2006, pp. 979-991

[6] Idiart, A., *et al.*, "A numerical and experimental study of aggregate-induced shrinkage cracking in cementitious composites," Cement and Concrete Research, Vol.42, No.2, 2012, pp. 272-281

[7] Kawai, T., "New discrete models and their application to seismic response analysis of structures," Nuclear Engineering and Design, Vol.48, No.1, 1978, pp. 207-229

[8] Yamamoto, Y., *et al.*, "Analysis of compression failure of concrete by three dimensional rigid body spring model," JSCE journal proceedings, Vol.64, No.4, 2008, pp. 612-630 (in Japanese)

[9] Sasano, H., *et al.*, "Impact of Drying on Structural Performance of Reinforced Concrete Shear Walls," Journal of Advanced Concrete Technology, Vol.16, No.5, 2018, pp. 210-232

[10] Scrivener, K.L., "The Interfacial Transition Zone (ITZ) Between Cement Paste and Aggregate in Concrete," Interface Science, Vol.12, No.4, 2004, pp. 411-421

[11] Lin, M., Itoh, M., and Maruyama, I., "Mechanism of Change in Splitting Tensile Strength of Concrete during Heating or Drying up to 90°C," Journal of Advanced Concrete Technology, Vol.13, No.2, 2015, pp. 94-102

[12] Bolander, J., *et al.*, "Rigid-Body-Spring Network modeling of cement-based composites," in *Fracture Mechanics of Concrete Structures*, R. de Borst, et al., Editors. 2001, AA Balkema: Lisse, The Netherlands. pp. 773-780.

[13] Kosaka, Y., Tanigawa, Y., and Oota, F., "Effect of coarse aggregate on fracture of concrete : Part 1 : Model Analysis," Transactions of the Architectural Institute of Japan, Vol.228, 1975, pp. 1-11,149 (in Japanese)

[14] JSCE, "Standard specifications for concrete structures -2002, inspection," 2002